PSEUDO-RANDOM HALFTONE SCREENING FOR COLOR AND BLACK&WHITE PRINTING.

Victor Ostromoukhov
Peripheral Systems Laboratory
Swiss Federal Institute of Technology (EPFL)
IN-F, CH-1015 Lausanne, Switzeland.

Abstract.

The idea of using pseudo-random spatial structures in graphic arts (color and black&white rendering algorithms) was suggested by psychologists and biologists about ten years ago. They observed that some natural pseudo-random structures such as the spatial distribution of receptors in the human retina play an important part in the perceptual process.

Our modelization of pseudo-random spatial structures resembles the retinal mosaic. It starts by obtaining the quasi-random distribution of tile centers according to some well-defined spectral characteristics. We then obtain the desired tesselation of the output device space by applying the Voronoi polygonization process.

Two slightly different approaches to the output image computation are being explored. In the first approach, an analytic black-dot curve is calculated according to the resampled input signal level and the area of each given tile. This analytic curve is scan-converted to obtain the blackened pixels. In the second approach, we associate threshold values to all pixels inside every tile according to some specially tailored analytic spot function. Then, the standard threshold comparison process is applied.

The quality of the obtained results is analysed using common techniques: the Fourier analysis and the human visual system model. The described halftone algorithm seems to be appropriate for high-resolution color and black&white devices (above 1000 dpi). For low- and medium-resolution devices (300 – 1000 dpi) some important limitations are discussed.

1. Introduction

In the printing industry, one of the most common methods for reproducing halftone images using bilevel printing devices is clustered-dot ordered dithering (see [Jud74], [Uli87]). This method consists in subdividing the whole output image space into repetitive adjoining rectangular areas – screen elements. The inside of each screen element is gradually blackened according to the gray level of the original image, thus ensuring the presence of various gray levels in the reproduction. The black dots are clustered in the middle of each screen element and form small rounded figures. The images produced using this method are quite faithful to the original and are visually pleasing.

Only rational angles are attainable with clustered-dot dithering, due to the discrete nature of the grids. This phenomenon can become harmful in the case of four-color printing, when different screen angles and maybe even different screen frequencies are used for separate color planes, thus producing a so-called Moiré phenomenon (see [Yul67], [Hun87], [Ami91], [Fin92]). In order to deal with this problem, most conventional RIPs (Raster Image Processors) try to approximate by rational angles either conventional angles ($15°, 45°, 75°$ and $0°$ for cyan, magenta, black and yellow color planes, respectively) or proprietary solutions such as Linotype-Hell screen/frequency combinations [Sch85].

The idea of using pseudo-random spatial mosaics in graphic arts (color and black&white rendering algorithms) was suggested by psychologists and biologists about ten years ago [Yel83]. They observed that some natural pseudo-random structures such as the spatial distribution of receptors in the human retina play an important part in the perceptual process. Fourier spectra of such structures show characteristic symmetrical well-distributed figures shaped as a ring or bell.
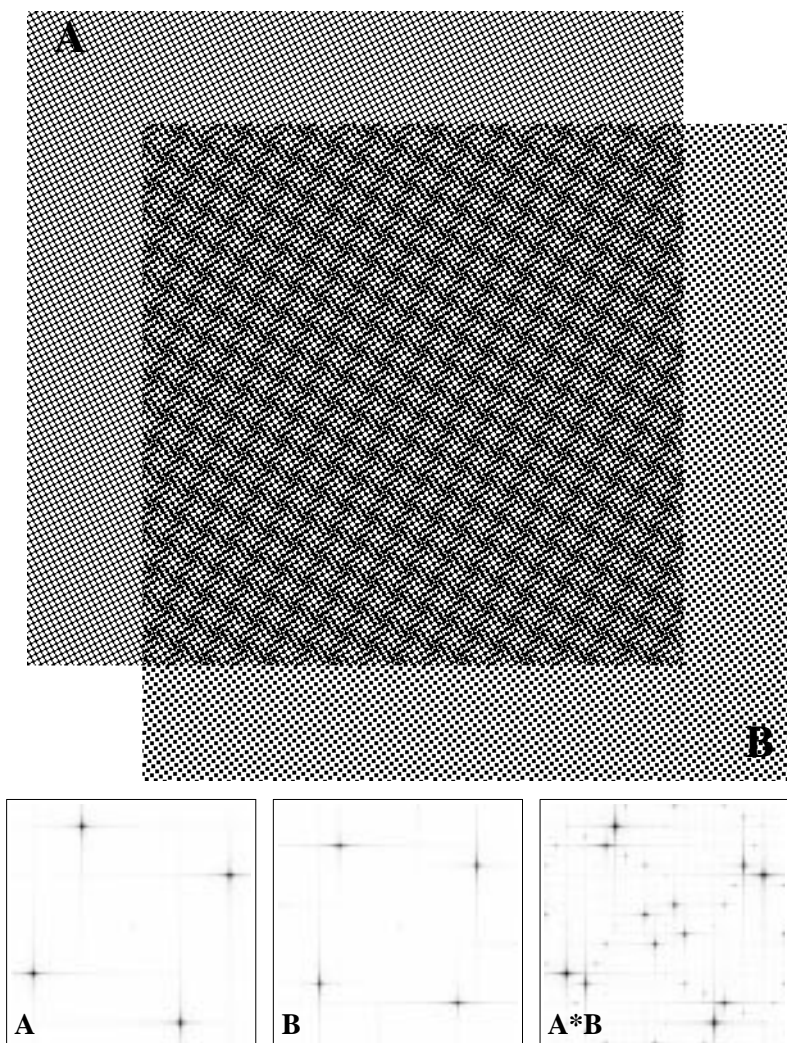
Fig. 1 Superimposition of two regular structures and their Fourier amplitude specrtra (the central part only).

This feature may be fruitfully exploited for building a system where two or more structures are to be superimposed. It is a well-known fact that when two structures are superimposed, the Fourier spectrum of the resulting structure is the convolution of two Fourier spectra of two images (superimposition is seen as a multiplication in the spatial domain which leads to the convolution in the spectral domain, see [Bra86]). Figures 1 and 2 illustrate this thesis: in the case of two regular superimposed structures A and B shown in figure 1a, the resulting Fourier spectrum shown in figure 1b has a new "parasite" frequency near the DC impulse – the phenomenon which is perceived as the Moiré fringe. In the case of two pseudo-random superimposed structures C and D shown in figure 2a, the resulting Fourier spectrum shown in figure 2b has no "parasite" Moiré frequency.

At low-resolution, different error-diffusion techniques with symmetrical spectra are widely used (see [Flo75], [Bil83], [Uli88]). Nevertheless, the error-diffusion technique cannot be used in conventional high resolution printing because of important dot gain due to ink spread. Such a printing process would become too difficult to control. Unlike the error-diffusion technique, the pseudo-random halftone screening technique can be applied in a high resolution printing process. Individual pixels in such a process are clustered, thus enabling fine control on dot gain and tone reproduction curve.

The phenomenon illustrated in figures 1 and 2 create a good basis for building an alternative solution to conventional regular screening for color printing purposes. Within the last two years, several commercial products using the pseudo-random structures have appeared on the market. We can mention, without any pretension to exhaustiveness, products such as Diamond Screening of Linotype-Hell or CristalRaster Screening of Agfa.
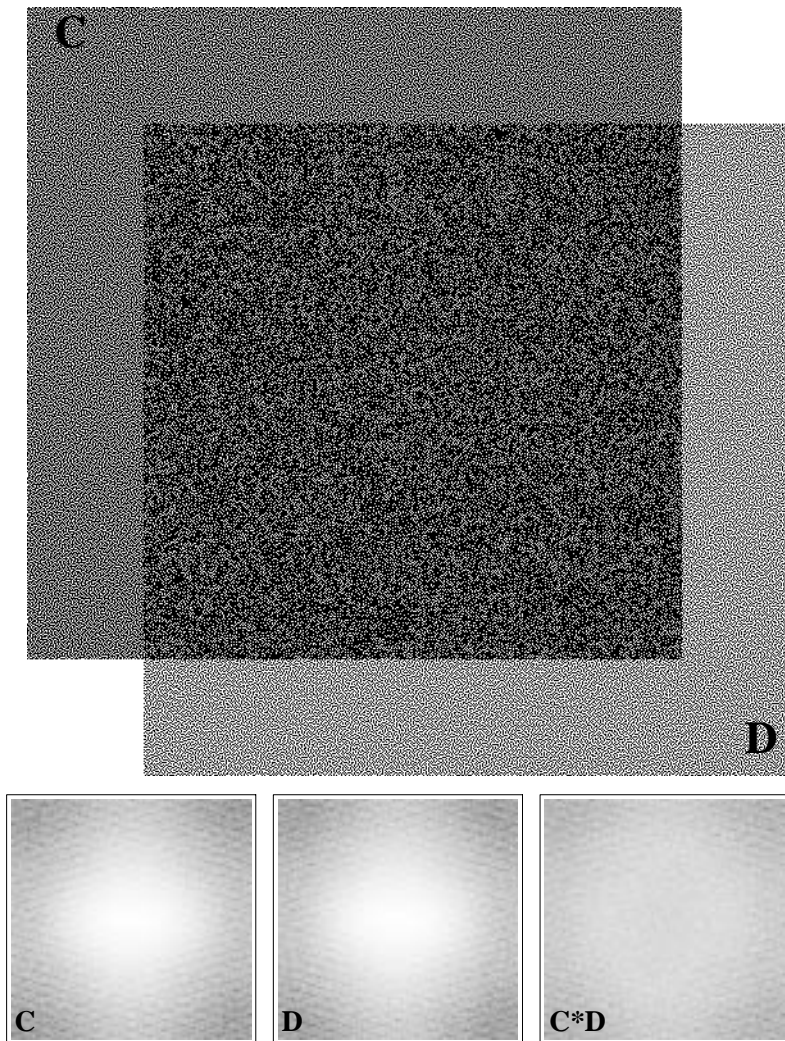
Fig. 2 Superimposition of two pseudo-random structures and their Fourier amplitude specrtra.

The goal of this paper is to show one possible way to build a system using pseudo-random structures, with all needed details. The presented method does not mimic any known commercial product and can be considered as an original contribution.

Our modelization of pseudo-random spatial structures starts from the pseudo-random distribution of tile centers obtained according to some well-defined rules. We then obtain the desired tiling of the output device space by applying the Voronoi polygonization process.

Two slightly different approaches to the output image computation are being explored. In the first approach, an analytic black-dot curve is calculated according to the resampled input signal level and the area of each tile. This analytic curve is scan-converted into a set of black and white pixels. In the second approach, we associate threshold values with all pixels inside every tile using a simple procedure. Then, the standard threshold comparison process is applied.

The quality of the obtained results is analysed using common techniques: the Fourier analysis and the human visual system model. The described halftone algorithm seems to be appropriate for high-resolution color and black&white devices (above 1000 dpi). For low- and medium-resolution devices (300 – 1000 dpi) some important limitations are discussed.

2. Pseudo-random tiling of the output device space

A screen element used in the standard ordered dithering technique is a regular tile which tiles the entire plane. Each individual cell of the screen element contains threshold values used during the image rendering process. The method described in this article uses a set of irregular pseudo-random tiles instead of regular tiles.

The first step in building pseudo-random tiling is to find a stochastic distribution of centers. There are different ways of obtaining such a distribution. One possible solution is an application of stochastic noise such as white or blue noise on perfectly distributed centers. In our modelization, we adopted another

model: we consider each center to be related to all its neighbours by a repulsive string (see figure 3) whose force is defined as follows

$$F = \frac{a}{r^k} \tag{1}$$

where r is the distance between two centers, k is the power law (we used values of k equals 3 and 4 in our modelization), and a is the string's strength. The neighbours are defined in the Voronoi sense.

At the beginning of the simulation, the centers are randomly distributed, as well as the strengths of the strings. We choose randomly to move one center; then we calculate the resulting force caused by all neighbours of the given center, and we calculate the displacement which is proportional and oriented in the sense of the resulting force. At this moment, the neighbours are recalculated, and the step is repeated with another center. After a certain number of iterations (which depends on the number of centers and the degree of initial randomness) the system becomes stable, and we freeze the thus obtained configuration of centers. Figure 4a shows a typical distribution of centers obtained with our model; its Fourier spectrum is shown in figure 4b.

The next step in our modelization is polygonization of the area covered by distribution of centers obtained at the previous stage using the well-known Voronoi polygonization process (see [Pre85]). The result of such a polygonization is shown in figure 4c. The entire center distribution process is rather time-consuming but it is calculated off-line; only the resulting Voronoi diagram is stored to be used in the image generation phase.
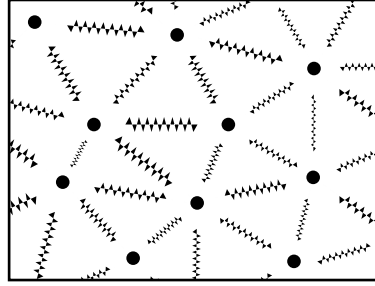
Fig. 3 Model of stochastic distribution of Voronoi polygons centers.

a)   b)   c)
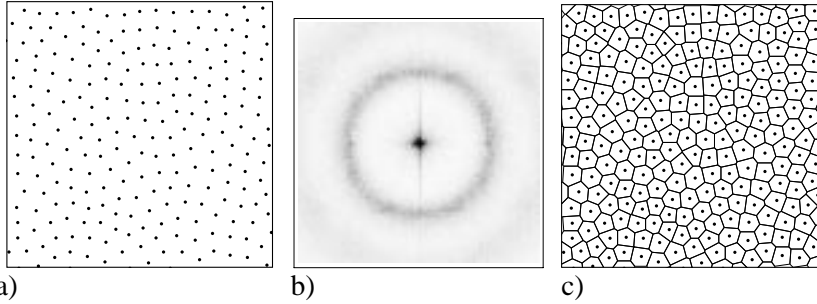
Fig. 4 Final distribution of Voronoi polygon centers (a); its Fourier amplitude spectrum (b) and the resulting Voronoi diagram (c).

3. Image generation. First approach: resampling

Once the output space is tiled with a set of pseudo-random Voronoi polygons, image generation can be performed using two different approaches. In the first approach, resampling, each Voronoi polygon is blackened according to the gray levels of input pixels surrounding the center of the polygon.

Resampling using linear (first order) approximation as well as cubic (third order) approximation is discussed in [Stu79]. Let f be a known linear transformation which relates input image space with output image space, and f^{-1} be an inverse transformation. For a given Voronoi polygon center (u, v) the corresponding input image coordinates $(x, y) = f^{-1}(u, v)$. Let $(i, j) = \text{floor}(x, y)$ be the integer part of the point (x, y). The gray values of four points $(i, j), (i + 1, j), (i, j + 1)$ and $(i + 1, j + 1)$ are known: $g(i, j), g(i + 1, j), g(i, j + 1)$ and $g(i + 1, j + 1)$, respectively. Consequently, one may easily calculate the gray level of the point (x, y) and of the corresponding point (u, v) using a standard linear approximation technique

$$g(x, y) = g(i, j) + \Delta x(g(i + 1, j) - g(i, j)) + \Delta y(g(i, j + 1) - g(i, j))$$
$$+ \Delta x \Delta y(g(i, j) - g(i + 1, j) - g(i, j + 1) + g(i + 1, j + 1)) \tag{2}$$

where $(\Delta x, \Delta y)$ is the difference between exact coordinates (x, y) and their truncated values (i, j):

$$(\Delta x, \Delta y) = (x, y) - \text{floor}(x, y)$$

The next step is the generation of a black dot pattern which corresponds to the gray level $g(x, y) = g(u, v)$ of a given Voronoi polygon. Our rasterization method consists in a) finding an analytical closed curve

whose area equals g times of the area of the Voronoi polygon under consideration; b) performing a vertical scan-conversion on the thus obtained analytical curve. The analytical closed curve described in this article consists of a set of straight line segments.

Let us take a look at figure 5. The polygon shown in figure 5a is a typical Voronoi polygon, with the center at point P_0 and vertices V_1, V_2, V_3, V_4, V_5 and V_6. The number N_s of neighbours surrounding the polygon under consideration, and consequently the number of sides of the polygon may be any number greater than 3 (the case of 6 neighbours represented in figure 5a is the most probable case). Points M_1, M_2, M_3, M_4, M_5 and M_6 designate midpoints between the center P_0 of the Voronoi polygon under consideration and centers P_1, P_2, P_3, P_4, P_5 and P_6 of surrounding polygons. The Voronoi polygon is subdivided in such a manner into $2N_s$ triangles, where N_s is the number of neighbours surrounding our Voronoi polygon. For explanation, let us consider only one triangle, e.g. $P_0V_1M_1$, as shown in figure 5b. Point A cuts the side V_1P_0 in proportion k

$$\frac{AP_0}{V_1A} = k \quad \implies \quad \frac{\text{Surface}(\Delta_{M_1AP_0})}{\text{Surface}(\Delta_{M_1V_1A})} = k \tag{3}$$

The global parameter k is fixed for all Voronoi polygons; its value defines the gray level limit between two cases: when black dots are grouped around the center P_0 and when white dots are grouped around vertices V_1, V_2, V_3, V_4, V_5 and V_6. In our modelization we obtained nice results with values of k which were either $2/3$ or $3/4$.

In order to generate appropriate analytical closed curve, let us draw two straight lines CD and EF parallel to M_1A

$$M_1A \parallel EF; \quad \frac{P_0F}{P_0A} = m \quad \implies \quad \frac{\text{Surface}(\Delta_{P_0EF})}{\text{Surface}(\Delta_{P_0AM_1})} = m^2 \tag{4}$$

$$M_1A \parallel CD; \quad \frac{V_1D}{V_1A} = n \quad \implies \quad \frac{\text{Surface}(\Delta_{V_1CD})}{\text{Surface}(\Delta_{V_1M_1A})} = n^2 \tag{5}$$

For a given gray level $g(x,y) \leq k$, we can calculate the $m = P_0F/P_0A$ ratio according to (4), for every triangle forming the given Voronoi polygon. The m ratio determines the analytical polygon to be scan-converted, as shown in figure 5c. For a gray level $g(x,y) > k$, we apply (5) in order to find the $n = V_1D/V_1A$ ratio; the result of such a calculation is shown in figure 5d.

Once the analytical curves delimiting black zones are found, we can perform standard vertical scan-conversion. The details of the vertical scan-conversion technique can be found in [Her88]. Black dots obtained in the scan-conversion process are put directly on the destination bitmap, at the appropriate place.

It is possible to conceive more sophisticated algorithms to calculate analytical curves for scan-conversion purposes. For example, the straight line segments can be replaced by Bézier curves. It is important to preserve area proportions which reflect the desired gray level $g(x,y)$. In this sense, our linear model is very simple and it is efficient enough.

It is natural to apply some extra corrections to compensate real device dot gain, non-linearity of human perceptual mechanism etc. A standard gamma-correction mechanism was used in our modelization. Figure 6 shows an image generated with the described technique.

4. Image generation. Second approach: thresholding

It is a well-known fact that images rendered with a resampling technique can lose precision when highly contrasted small details are visualized. Instead, most rendering techniques perform partial dot screening and preserve little details by applying dither thresholding (see [Fin92]).

The technique described in the previous section can be improved by replacing the resampling technique by a pseudo-random non-standard thresholding technique.

Let us briefly recall the conventional thresholding technique. For every pixel (x,y) of the source image, the gray level $g(x,y)$ is known. The linear transformation f transforms a unit square of the source image into a rectangular zone, in the output device space. The thresholding algorithm takes into consideration *each* individual pixel inside the destination rectangle and compares the value g with pre-calculated threshold values. If g is greater than the threshold value, the destination pixel is black; otherwise, it is white. Only one repetitive threshold matrix is stored, and all calculations related to the algorithm (pixel position calculation, camparison etc.) are performed on the fly.

The pseudo-random non-standard thresholding technique uses the same basic principle as the conventional thresholding technique; the only difference consists in finding pre-calculated threshold values.
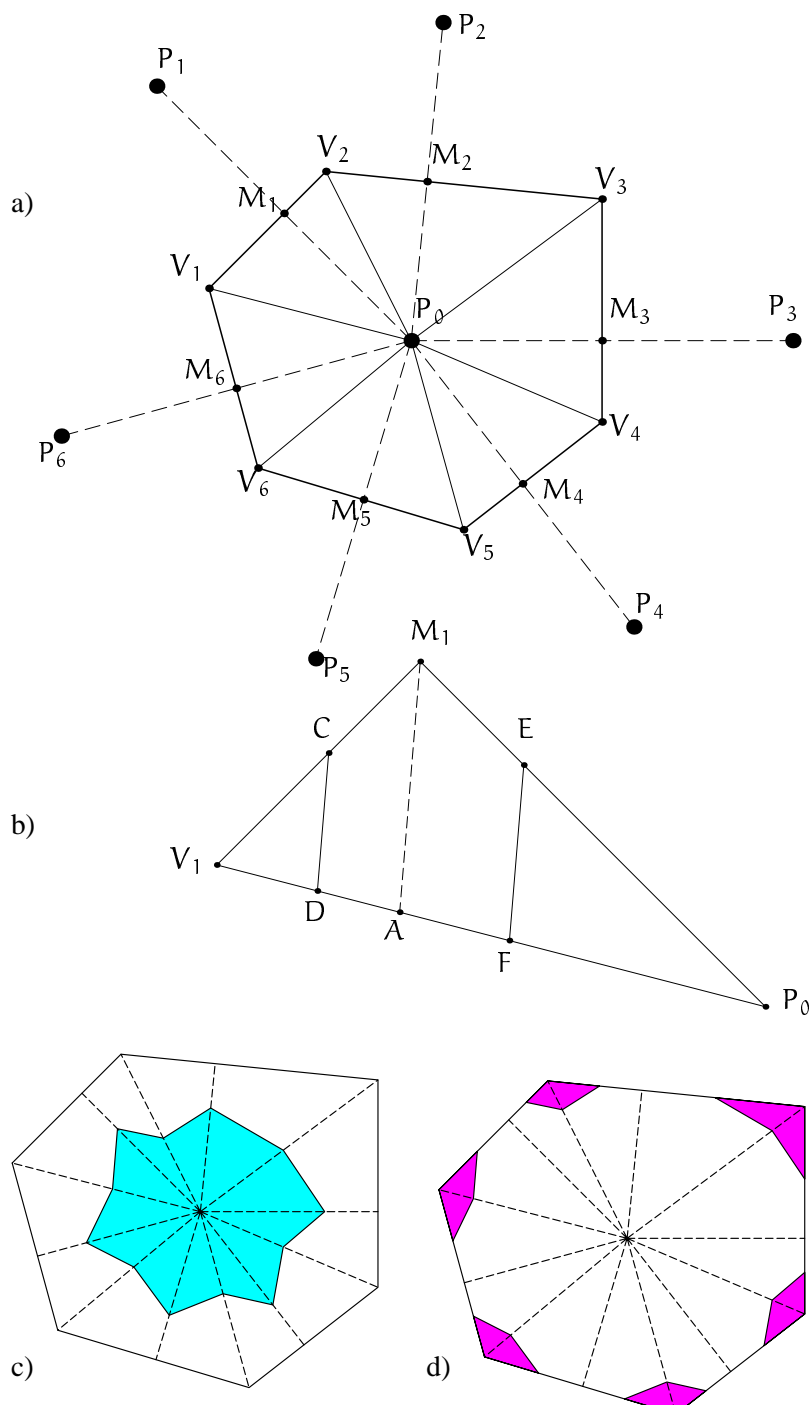
Fig. 5 Typical Voronoi polygon (a), significant triangle (b), resulting analytical curve in the case where $g(x,y) \leq k$ (c) and in the case where $g(x,y) > k$ (d).

In general, if all Voronoi domains discussed in the previous section are different, all Voronoi domains with their associated threshold values have to be stored. Nevertheless, for practical purposes, one can considerably diminish the amount of storage by a) replacing floating-point values of Voronoi diagram vertices by integer values; b) sorting all possible configurations by applying the vertex coordinates difference criterion. In such a case, not only the amount of storage diminishes, but processing time also decreases because the access to a sorted multi-dimensional array is fast enough.

Filling the Voronoi polygon with appropriate threshold values is a relatively simple task. To do it, rendering cycle described in the previous section must be repeated for all gray levels varying from 0 up to 255 (or up to another maximum gray level). For any individual pixel inside the Voronoi polygon, the associated threshold value is the gray level at which the pixel becomes black. Once all threshold values inside Voronoi polygon are set the polygon can be stored. Because it is time-consuming, this calculation should be performed off-line.

Except in the case of fine detail rendering, the overall image quality is very similar to the quality obtained with the resampling technique described in the previous section.

6

Fig. 6 Typical image produced with the pseudo-random halftone screening technique, output at low resolution (300 dpi). The target output device should be at least 2000 dpi.

5. Discussions and Conclusions

The pseudo-random halftone screening technique described in this article can be used to faithfully reproduce gray scale images while guaranteeing the desired spectral characteristics. Fourier spectra of bilevel images rendered with this technique have symmetrical well-distributed figures shaped as a ring or bell. When such a rendering technique is applied in the color printing process, the Moiré effect can be avoided. Other possible application domains of pseudo-random halftone screening are fax machines, scanners and other regular-matrix raster devices.

Unlike known error-diffusion techniques, the pseudo-random halftone screening technique can be applied in a high resolution printing process. The characteristic screen element size can be properly chosen so as to ensure the best trade-off between the printing process constraints and the most precise printing. Appropriate gamma correction should be carried out in order to compensate the printing device dot gain, non-linearity of human perceptual mechanism etc.

At low and medium resolution, the technique described in this article produces a too coarse grain. In addition, human perceptual mechanism detects local structures which are not reflected in the standard Fourier analysis (see [Kel90]). This effect leads to perceiving non-existing structures like long oscillating chains when individual screen elements are clearly visible. Not only individual screen elements but even small groups of screen elements should be beyond our visual acuity limit – it is clearly the case in conventional photography; it can also be achieved in high quality high resolution printing. Consequently, conventional error-diffusion techniques are probably better for low and medium resolution rendering except in the case of some special applications where a coarse grain effect is desired.

We conclude that the pseudo-random halftone screening technique might take the same place in high-resolution rendering as the conventional error-diffusion technique has in low and medium resolution rendering, i.e. in rendering where specific symmetrical well-distributed Fourier spectra of obtained images are required.

6. Acknowledgements

7. References

[Ami91] I. Amidror. The moiré phenomenon in colour separation. Proceedings of the RIDT'91 Conference, Boston, Cambridge University Press, pp. 98-119, 1991.

[Bil83] C. Billotet-Hoffmann, O. Bryngdahl. On the error diffusion technique for electronic halftoning. *Proceedings of the SID,* 24(3), pp.253-258, 1983.

[Bra86] R.N. Bracewell. *The Fourier transform and its applications.* McGraw-Hill, 1986.

[Fin92] Fink, P., *PostScript Screening: Adobe Accurate Screens.* Adobe Press, 1992.

[Flo75] Floyd, F. & Steinberg, L., An Adaptive Algorithm for Spatial Grey Scale. *SID International Symposium Digest of Technical Papers,* Vol. VI, pp. 36-37, 1975.

[Her88] R.D. Hersch. Vertical scan-conversion for filling purposes. *Proceedings CGI'88,* Springer Verlag, pp. 318-327, 1988.

[Hun87] R.W.G. Hunt. *The reproduction of colour.* Fountain Press, 1987.

[Jud74] Judice, J.N., J.F.Jarvis, W.Ninke, "A Survey of Techniques for the Image Display of Continuous Tone Pictures on Bilevel Displays", *CGIP,* 5(1), March 1976, pp. 13-40.

[Kel90] Kelly, D.H., Retinocortical processing of spatial patterns. *Human Vision and Electronic Imaging: Models, Methods and Applications.* SPIE Vol. 1249. (eds. B.E. Rogowitz and J.P. Allebach) pp. 90-117. 1990.

[Pre85] F.P. Preparata, M.I. Shamos. *Computational Geometry.* Springer-Verlag, 1985.

[Sch81] Schoppmeyer, J., Screen Systems for Multicolor Printing. *European Patent No. 81109796.3,* (1981).

[Stu79] P. Stucki. Image processing for document reproduction. *Advances in digital image processing,* Plenum Press, N.Y., 1979.

[Uli87] R. Ulichney. *Digital Halftoning.* The MIT Press, 1987.

[Uli88] R.A. Ulichney. Dithering with blue noise. *Proceedings of the IEEE,* 76(1), pp.56-61, 1988.

[Yel83] J.I. Yellott, Jr. Spectral consequences of photoreceptor sampling in the rhesus retina. Science, Vol.221, pp. 382-385, 1983.

[Yul67] J.A.C. Yule. *Principles of Color Reproduction.* John Wiley & Sons, New York, 1967.